Available online at www.sciencedirect.com
SCIENCE DIRECT®
Inorganica Chimica Acta 350 (2003) 93–100
Inorganica Chimica Acta
www.elsevier.com/locate/ica

Influence of the bridging ligand on the substitution chemistry of neutral and cationic triruthenium carbonyl cluster complexes derived from 1,1-dimethylhydrazine

Javier A. Cabeza [a,*], Ignacio del Río [a], Santiago García-Granda [b], Lorena Martínez-Méndez [a], Víctor Riera [a]

[a] Departamento de Química Orgánica e Inorgánica, Instituto de Química Organometálica "Enrique Moles", Universidad de Oviedo-CSIC, E-33071 Oviedo, Spain
[b] Departamento de Química-Física y Analítica, Universidad de Oviedo, E-33071 Oviedo, Spain

Received 3 May 2002; accepted 3 June 2002

Dedicated to Professor Pierre Braunstein, an outstanding organometallic cluster chemist.

Abstract

The reactivity of the neutral triruthenium carbonyl cluster $[Ru_3(\mu\text{-}H)(\mu_3\text{-}HNNMe_2)(CO)_9]$ (**1**) and its protonated derivative $[Ru_3(\mu\text{-}H)_2(\mu_3\text{-}HNNMe_2)(CO)_9][BF_4]$ (**2**), both containing a face-capping 5-electron donor 1,1-dimethylhydrazido ligand, with triphenylphosphane has been studied. Compound **1** gives a mixture of two non-interconvertible isomeric carbonyl substitution products $[Ru_3(\mu\text{-}H)(\mu_3\text{-}HNNMe_2)(CO)_8(PPh_3)]$ which bear the phosphane ligand attached to the same Ru atom as either the NMe_2 (**3a**) or the NH fragments (**3b**). Protonation of the **3a** and **3b** mixture with $[HOEt_2][BF_4]$ gives a mixture of two non-interconvertible isomeric cationic dihydrido derivatives $[Ru_3(\mu\text{-}H)_2(\mu_3\text{-}HNNMe_2)(CO)_8(PPh_3)][BF_4]$ (**4a** and **4b**) which maintain the phosphane ligand in the same position as their neutral precursors. Compound **4a** can be selectively prepared from complex **2** and triphenylphosphane. Deprotonation of complex **4a** with triethylamine gives compound **3a**, selectively. These results contrast with those previously known for carbonyl substitution reactions on triruthenium clusters isostructural with compounds **1** and **2** but containing other face-capping five-electron donor ligands. The hardness of the bridging ligand is presented as an important factor in relation to the observed regioselectivity. The X-ray structures of compounds **2** and **4a** are reported.

Keywords: Ruthenium; Ruthenium clusters; Carbonyl substitution reactions; 1,1-Dimethylhydrazine; Crystal structures

1. Introduction

The substitution of a phosphane ligand for a CO ligand in carbonyl metal clusters is a common reaction [1]. However, despite the great number of such reactions reported to date, for a given cluster complex, the precise coordination site that is prone to undergo a carbonyl substitution cannot be predicted in many occasions, since it seems to be strongly influenced by the cluster structure and by the remaining ligands of the complex.

In this field, we have previously reported the carbonyl substitution chemistry of the cluster complexes $[Ru_3(\mu\text{-}H)(\mu_3\text{-}HNCONMe_2)(CO)_9]$ (**A**) [2], $[Ru_3(\mu\text{-}H)(\mu_3\text{-}ampy)(CO)_9]$ (**B**; Hampy = 2-amino-6-methylpyridine) [3–7] and the protonated derivative $[Ru_3(\mu\text{-}H)_2(\mu_3\text{-}ampy)(CO)_9][BF_4]$ (**C**) [3–7] (Scheme 1). These compounds contain face-capping five-electron donor ligands attached to the three ruthenium atoms through two heteroatoms. Without exceptions, complexes **A**–**C** un-

* Corresponding author. Tel.: +34-98-5103 501; fax: +34-98-5103 446.
E-mail address: jac@sauron.quimica.uniovi.es (J.A. Cabeza).

0020-1693/02/$ - see front matter © 2002 Elsevier Science B.V. All rights reserved.
doi:10.1016/S0020-1693(02)01493-7

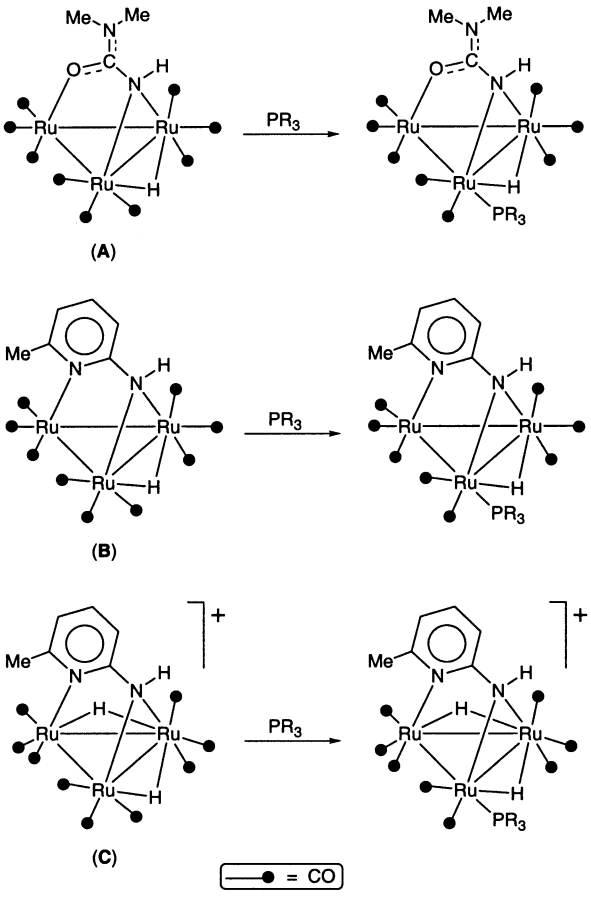

Scheme 1.

dergo substitution of a phosphane ligand for a CO ligand at an equatorial site on a ruthenium atom attached to both a hydride and the amido fragment of the bridging ligand (Scheme 1). This regioselectivity has been associated with the *cis*-labilizing effect provoked by the hardness of both the amido and hydride ligands [3,4].

In 1990, Süss-Fink et al. published the synthesis of several triruthenium carbonyl derivatives of the type $[Ru_3(\mu\text{-}H)(\mu_3\text{-}HNNR^1R^2)(CO)_9]$ by treatment of $[Ru_3(CO)_{12}]$ with hydrazines [8]. To date, no phosphane derivative chemistry of these cluster complexes has been reported. These compounds are isostructural with complexes **A** and **B**, but their face-capping five-electron donor ligands are hydrazido fragments, which are harder than ureato and 2-amidopyridine fragments. This fact prompted us to study the CO substitution chemistry of $[Ru_3(\mu\text{-}H)(\mu_3\text{-}HNNMe_2)(CO)_9]$ (**1**) and its protonated derivative $[Ru_3(\mu\text{-}H)_2(\mu_3\text{-}HNNMe_2)(CO)_9][BF_4]$ (**2**), in order to compare it with that known for the derivatives **A**–**C** and to draw some conclusions on the influence of ligand electronic factors (hardness) in the regioselectivity of CO substitution reactions by phosphane ligands on carbonyl cluster complexes.

2. Results and discussion

2.1. Synthesis of compounds 1 and 2

The compound $[Ru_3(\mu\text{-}H)(\mu_3\text{-}HNNMe_2)(CO)_9]$ (**1**) was prepared from $[Ru_3(CO)_{12}]$ and 1,1-dimethylhydrazine, as described by Vahrenkamp [9], using a modification of the general method proposed by Süss-Fink et al. for the synthesis of other hydrazido derivatives of $[Ru_3(CO)_{12}]$ [8]. Its IR and ^{1}H NMR spectroscopic data are given in Tables 1 and 2, respectively, in order to allow comparisons with the spectra of its derivatives. The use of 1,1-dimethylhydrazine was decided because the presence of two methyl groups on the same nitrogen atom would lead to a symmetric triruthenium derivative, with a statistically simpler regioreactivity than that of asymmetric derivatives, and with reaction products easily traceable by ^{1}H NMR.

Protonation of compound **1** with $[HOEt_2][BF_4]$ in dichloromethane afforded the cationic derivative $[Ru_3(\mu\text{-}H)_2(\mu_3\text{-}HNNMe_2)(CO)_9][BF_4]$ (**2**) in quantitative yield (Scheme 2). Its room temperature ^{1}H NMR spectrum showed only three singlet resonances (Table 2), assignable to the N*H* proton, the methyls and the hydrides, suggesting a C_S symmetry for the complex. This surprised us because the related complex $[Ru_3(\mu\text{-}H)_2(\mu_3\text{-ampy})(CO)_9][BF_4]$ (**C**) is asymmetric both in the solid state and in solution at room temperature [3]. In addition, the carbonyl region of its IR spectrum (Table 1), that is comparable with that of **C** [3], showed the ν(CO) absorptions shifted to higher wavenumbers than those of complex **1**, as expected for a higher formal oxidation state of the metal atoms.

An X-ray diffraction study, commented below, determined that compound **2** is asymmetric in the solid state and suggested that the complex might be stereochemically non rigid in solution. This was confirmed by a variable temperature ^{1}H NMR study, from which a small activation $\Delta G^{\ddagger}$ parameter of 9.1 kcal mol^{-1} was estimated from the coalescence temperature [10]. Fig. 1

Table 1
Selected IR data for the new complexes

Compound	ν(CO) (cm^{-1})
1 [a]	2079 (m), 2049 (s), 2021 (s), 2001 (m), 1958 (w), 1942 (w)
2 [b]	2138 (m), 2102 (s), 2085 (s), 2067 (m), 2039 (m), 2027 (m)
3a [b]	2061 (m), 2023 (s), 1999 (m), 1979 (m), 1958 (m)
3b [b,c]	1984 (m), 1930 (w)
4a [b]	2130 (m), 2082 (s), 2059 (m), 2031 (m), 2003 (m), 1957 (m)
4b [b,d]	2100(w), 2074 (s), 2020 (m)

[a] In THF.
[b] In CH_2Cl_2.
[c] Data extracted from the spectrum of a 1:1 mixture of **3a** and **3b**; only the absorptions that do not overlap with those of **3a** are given.
[d] Data extracted from the spectrum of a 1:1 mixture of **4a** and **4b**; only the absorptions that do not overlap with those of **4a** are given.

Table 2
^{1}H and ^{31}P NMR data for the new complexes[a]

Complex	^{1}H NMR				$^{31}P\{^{1}H\}$ NMR
	NH	Me_2	μ-H	PPh_3	
1 [b]	4.87 (s)	2.62 (s)	−13.06 (s)		
2 [c]	7.32 (s)	3.00 (s)	−14.71 (s)		
3a [b]	4.77 (s)	2.53 (s), 1.77 (s)	−12.25 (d) {10.3}	7.55 (m)	26.9 (s)
3b [b,d]	4.88 (s)	2.53 (s)	−12.00 (d) {9.8}	7.55 (m)	33.8 (s)
4a [c]	7.07 (s)	3.06 (s), 2.31 (s)	−13.78 (t) [3.1] {3.1}, −14.60 (dd) [3.1] {9.3}	7.52 (m)	27.3 (s)
4b [c,e]	7.28 (s)	3.06 (s)	−12.90 (d) {6.0}, −15.22 (d) {7.9}	7.50 (m)	41.0 (s)

[a] Spectra run at room temperature; multiplicities are given in parentheses; coupling constants are given within square brackets [$J_{(H-H)}$] or braces {$J_{(H-P)}$} in Hz.
[b] In $CDCl_3$.
[c] In CD_2Cl_2.
[d] Data extracted from the spectrum of a 1:1 mixture of **3a** and **3b**.
[e] Data extracted from the spectrum of a 1:1 mixture of **4a** and **4b**.

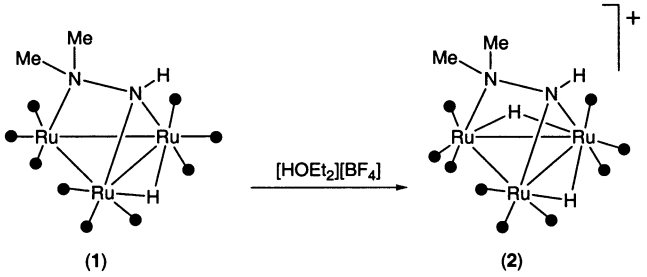

Scheme 2.

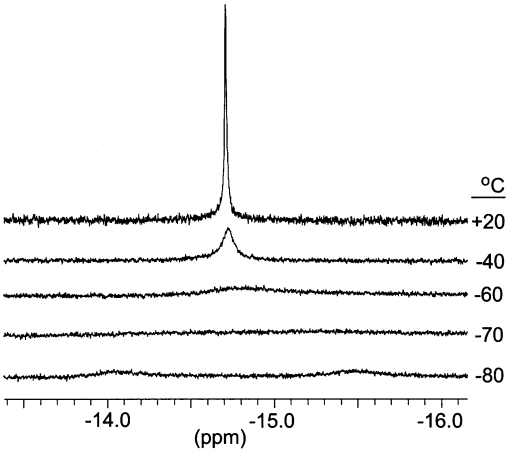

Fig. 1. Variable temperature ^{1}H NMR spectra of compound **2** in the hydride region (400 MHz, CD_2Cl_2).

shows that the fluxional process was not completely frozen at −80 °C, at which two individual hydride peaks start to become apparent (−14.1 and −15.5 ppm). The same effect is observed for the methyls of the NMe_2 group. We have found no reasons that could account for the high fluxionality of complex **2** as compared with the rigidity of complex **C**.

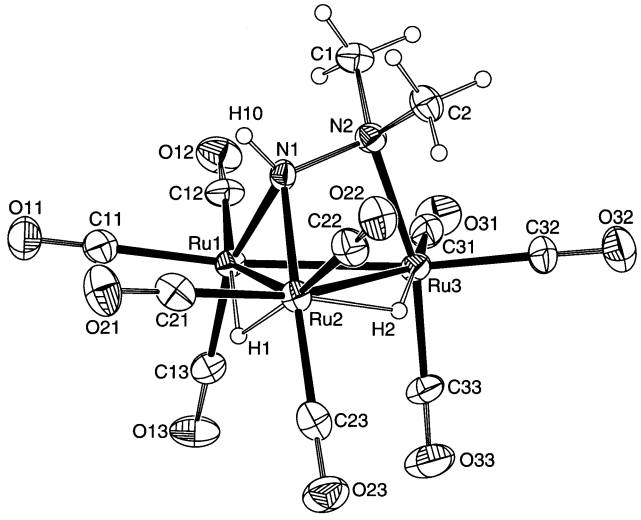

Fig. 2. Structure of the cationic part of compound **2** (only one of the two independent cations found in the solid is shown). Ellipsoids are drawn at the 50% probability level.

Fig. 2 shows a view of complex **2** in the solid state. A selection of bond lengths and angles for the two crystallographically independent clusters found in the crystals is given in Table 3. The cation can be described as a triangle of ruthenium atoms bonded to nine CO groups (three to each metal atom) and to the nitrogen atoms of a 1,1-dimethylhydrazido ligand. While the NH fragment of this ligand bridges the Ru(1)–Ru(2) edge, the NMe_2 fragment is attached to the Ru(3) atom. Two hydride ligands span the Ru(1)–Ru(2) and Ru(2)–Ru(3) edges. The three axial CO ligands are approximately *trans* to the N–Ru bonds, while two of the six equatorial CO ligands are colinear with the Ru(1)–Ru(3) edge and the remaining four are *trans* to the hydride ligands. This structure reminds that of cluster **C** [3].

Table 3
Selected interatomic distances (Å) in **2a**, **2b** and **4a** [a]

	2a	2b	4a
Ru(1)–Ru(2)	2.7624(8)	2.7801(8)	2.7828(7)
Ru(1)–Ru(3)	2.7315(8)	2.7445(8)	2.7422(8)
Ru(2)–Ru(3)	2.9544(8)	2.9486(8)	2.9702(7)
Ru(1)–N(1)	2.102(6)	2.103(7)	2.106(6)
Ru(2)–N(1)	2.096(7)	2.101(7)	2.105(6)
Ru(3)–N(2)	2.176(6)	2.182(7)	2.202(5)
Ru(3)–P(1)	–	–	2.406(2)
Ru(1)–C(11)	1.966(10)	1.964(9)	1.951(8)
Ru(1)–C(12)	1.891(8)	1.903(10)	1.904(8)
Ru(1)–C(13)	1.904(8)	1.916(10)	1.900(8)
Ru(2)–C(21)	1.934(10)	1.923(8)	1.933(8)
Ru(2)–C(22)	1.953(10)	1.967(10)	1.944(8)
Ru(2)–C(23)	1.937(10)	1.920(9)	1.941(8)
Ru(3)–C(31)	1.912(9)	1.895(9)	1.873(8)
Ru(3)–C(32)	1.934(9)	1.969(10)	–
Ru(3)–C(33)	1.905(8)	1.899(10)	1.861(7)
Ru(1)–H(1)	1.77(7)	1.85	1.77(5)
Ru(2)–H(1)	1.53(7)	1.85	1.70(5)
Ru(2)–H(2)	1.71(8)	1.83(7)	1.74
Ru(3)–H(2)	1.69(8)	1.86(7)	1.73
N(1)–N(2)	1.473(8)	1.457(9)	1.462(7)
C(1)–N(2)	1.485(10)	1.474(12)	1.495(8)
C(2)–N(2)	1.499(10)	1.488(11)	1.491(8)
C(11)–O(11)	1.135(11)	1.120(11)	1.130(9)
C(12)–O(12)	1.140(10)	1.138(11)	1.132(8)
C(13)–O(13)	1.128(10)	1.135(12)	1.144(8)
C(21)–O(21)	1.129(11)	1.122(10)	1.138(8)
C(22)–O(22)	1.115(11)	1.117(11)	1.117(8)
C(23)–O(23)	1.120(11)	1.141(11)	1.112(8)
C(31)–O(31)	1.128(11)	1.137(11)	1.139(8)
C(32)–O(32)	1.142(10)	1.118(11)	–
C(33)–O(33)	1.114(11)	1.134(11)	1.146(8)

[a] **2a** and **2b** are the two independent molecules found in the asymmetric unit of compound **2**.

2.2. Reactivity of complex *1* with triphenylphosphane

No reaction was observed when complex **1** was treated with 1 equiv. of triphenylphosphane in THF at room temperature. After 30 min at reflux temperature, an approximately 50% mixture (estimated by ^{1}H NMR integration) of two isomeric monosubstituted derivatives, **3a** and **3b**, of formula $[Ru_3(\mu\text{-}H)(\mu_3\text{-}HNNMe_2)(CO)_8(PPh_3)]$ was obtained (Scheme 3). This mixture could not be separated. Longer reaction times at reflux temperature did not change the ratio of the complexes, indicating that they do not interconvert. Their ^{1}H NMR spectrum showed their hydrides as doublets (Table 2) with $J_{(P-H)}$ coupling constants of approximately 10 Hz, typical of *cis* P-hydride arrangements [2–7]. Interestingly, the phosphane ligand affects strongly the methyls of the NMe_2 group only in complex **3a**, for which two distinct methyl resonances are clearly observed, while both methyl groups of isomer **3b** appear at the same chemical shift. All these data strongly support the structures depicted in Scheme 3 for these complexes,

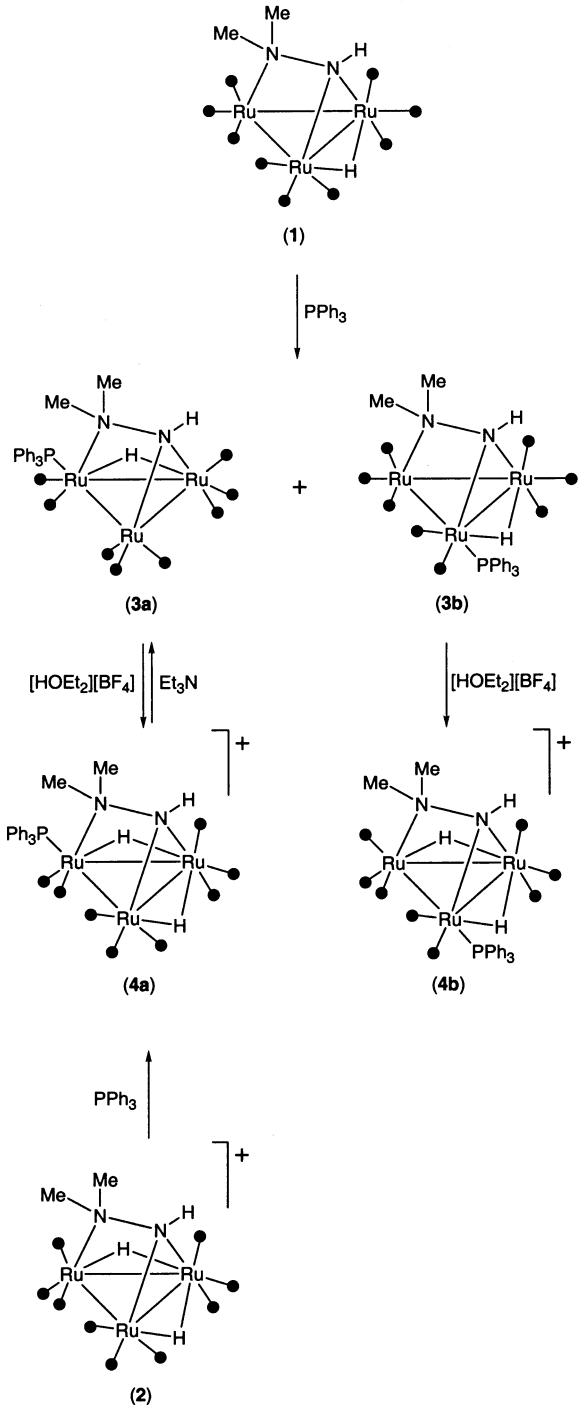

Scheme 3.

which bear the phosphane ligand attached to the same Ru atom as either the NMe_2 (**3a**) or the NH fragments (**3b**). In the case of complex **3a**, the carbonyl substitution process is accompanied by an edge to edge migration of the hydride ligand. Pure **3a** was subsequently obtained by deprotonation of the cationic complex **4a** (vide infra), in which the phosphane ligand is also attached to the same Ru atom as the NMe_2 group.

These results contrast with those known for the reactions of clusters **A** and **B** with triphenylphosphane, since those reactions are instantaneous at room temperature and render only one substitution product (the one analogous to **3b**) [2,3]. In carbonyl cluster chemistry, carbonyl substitution processes preferentially occur in coordination sites *cis* to hard ligands [2–7]. Therefore, it seems that both nitrogen atoms of the dimethylhydrazido ligand possess a similar *cis*-labilizing effect, probably as a consequence of a parallel hardness. However, in the case of compounds **A** and **B**, their NH fragments are clearly harder than the ketonic fragment of **A** or the pyridine fragment of **B**, which are involved in π-bonding, and this accounts for the regioselectivity of their substitution reactions.

2.3. Reactivity of complex 2 with triphenylphosphane

The cationic character of complex **2** should enhance the cluster reactivity toward nucleophilic reagents, promoting carbonyl substitutions and/or nucleophilic additions. In fact, complex **2** reacted slowly with 1 equiv. of triphenylphosphane at room temperature to give the substituted derivative $[Ru_3(\mu\text{-}H)_2(\mu_3\text{-}HNNMe_2)(CO)_8(PPh_3)][BF_4]$ (**4a**) (Scheme 3). However, the reaction was more conveniently carried out at reflux temperature (THF) in order to reduce the reaction time to 20 min.

In the ^1H NMR spectrum of **4a** (Table 2), it was observed that both hydride ligands were coupled to each other ($J = 3.1$ Hz) and to the phosphorus atom. From the values of the $J_{(H-P)}$ coupling constants (9.3 and 3.1 Hz), it was inferred that the phosphane ligand is *cis* to a hydride and far away from the other. With the analytical and spectroscopic data of **4a** it was not possible to unequivocally assign its structure, which was determined by X-ray diffraction methods.

The structure of compound **4a** (Table 3, Fig. 3) is entirely analogous to that of **2**, except for the presence of a triphenylphosphane ligand, attached to the same Ru atom as the NMe_2 fragment, in an equatorial position *cis* to the bridging hydride.

Again, this result differs from that previously known for the analogous ampy derivative **C**, for which its substitution product contains the phosphane ligand attached to the Ru atom bonded to the NH fragment and to only one hydride [3].

The fact that compound **4a** is the only product obtained in the reaction of complex **2** with triphenylphosphane indicates that the protonation of **1** increases the electrophilic character of the Ru atom attached to NMe_2 fragment to a greater extent than those of the other two Ru atoms. In contrast, the softness of the pyridyl fragment of complex **C** makes the Ru atom to which it is bonded less electrophilic than the amido-bonded Ru atoms and this accounts for the observed reactivity (Table 4).

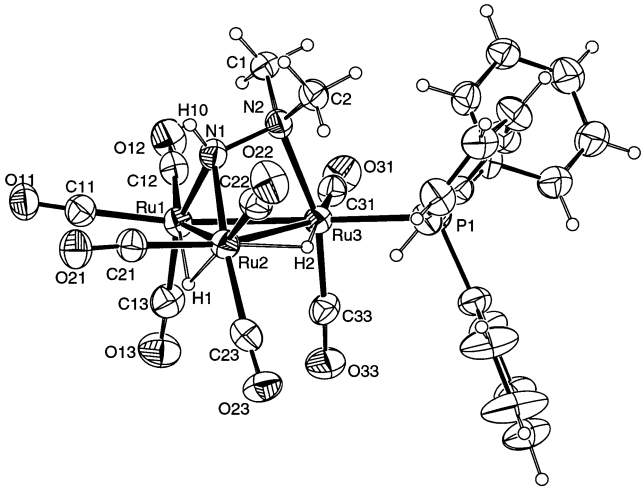

Fig. 3. Structure of the cationic part of compound **4a**. Ellipsoids are drawn at the 50% probability level.

2.4. Protonation and deprotonation reactions

As outlined in Scheme 3, complex **4a** could be deprotonated with triethylamine to give the neutral derivative **3a**. This provided an appropriate synthetic method to make complex **3a** in a pure form, since treatment of **1** with triphenylphosphane afforded an inseparable mixture of the isomers **3a** and **3b** (vide supra). In addition, protonation of this mixture with $[HOEt_2][BF_4]$ in dichloromethane led to a mixture of the cationic dihydrido derivatives **4a** and **4b**. The ratio of these complexes remained unaltered after heating the mixture in refluxing THF for 1 h, therefore, they do not interconvert. Although compound **4b** could not be prepared free of **4a**, its ^1H and ^{31}P NMR spectroscopic data (Table 2) were obtained from the spectra of the mixture. The $J_{(H-P)}$ coupling constants of its hydride resonances (7.9 and 6.0 Hz) clearly indicate that the phosphorus atom is not *trans* to any of the hydrides, since $J_{(H-P)}$ values greater than 20 Hz are expected for this situation [3,4]. Consequently, the position of the phosphane ligand in **4b** is that depicted in Scheme 3.

All these data indicate that the atom connectivity is maintained in the protonation and deprotonation reactions.

3. Conclusions

The systematic study reported herein and the comparison of the obtained results with those known for

Table 4
Crystal data and structure refinement details for compounds **2** and **4a**

	2	**4a**
Formula	$C_{11}H_9BF_4N_2O_9Ru_3$	$C_{28}H_{24}BF_4N_2O_8PRu_3$
Formula weight	703.22	937.48
Crystal system	triclinic	monoclinic
Space group	$P\bar{1}$	$C2/c$
a (Å)	8.3735(3)	36.271(3)
b (Å)	16.4026(7)	12.4706(7)
c (Å)	16.9120(7)	16.5046(11)
α (°)	63.659(2)	90
β (°)	89.286(3)	112.296(3)
γ (°)	79.993(2)	90
V (Å^3)	2044.7(1)	6907.3(8)
Z	4	8
$F(000)$	1336	3664
D_{calc} (g cm^{-3})	2.284	1.803
Radiation (λ, Å)	Cu Kα (1.54180)	Cu Kα (1.54180)
μ (mm^{-1})	18.508	11.550
Crystal size (mm)	0.20 × 0.02 × 0.02	0.18 × 0.13 × 0.10
Temperature (K)	200(2)	200(2)
θ Limits (°)	2.92–68.91	3.78–68.61
Min/max h, k, l	0/10, −19/19, −20/20	0/43, −15/15, −19/18
Number of reflections collected	33 775	12 311
Unique reflections (R_{int})	7540 (0.083)	6352 (0.076)
Reflections with $I > 2\sigma(I)$	6107	4508
Absorption correction	RefDelF (XABS2)	RefDelF (XABS2)
Max/min transmission	0.478/0.212	0.315/0.221
Parameters, restraints	356, 2	436, 0
Goodness-of-fit on F^2	1.088	1.030
Final R_1 (on F, $I > 2\sigma(I)$)	0.0473	0.0543
Final wR_2 (on F^2, all data)	0.1615	0.1505
Min/max residuals (e Å^{-3})	−1.142/1.695	−0.715/1.037

analogous carbonyl substitution reactions on structurally related triruthenium clusters containing other face-capping ligands allow the conclusion that the regioselectivity of the reactions is more influenced by electronic factors associated with the bridging ligands than by structural factors, since structurally related compounds displayed different reactivity. The entering phosphane ligand ends *cis* to a hydride ligand in an equatorial site attached to the most electrophilic metal atom, which is generally bonded to the hardest fragment of the bridging ligand.

Although hardness may account (at least to a considerable extent) for the observed regioselectivity, we have found no reasonable relationship between ligand hardness and the milder conditions required for the reactions of **A**–**C** relative to those required by **1** and **2**.

4. Experimental

4.1. General data

Solvents were dried over sodium diphenyl ketyl (THF, diethyl ether hydrocarbons) or CaH_2 (dichloromethane, 1,2-dichloroethane) and distilled under nitrogen prior to use. The reactions were carried out under nitrogen, using Schlenk-vacuum line techniques, and were routinely monitored by solution IR spectroscopy and by spot TLC. All reagents were purchased from commercial suppliers. IR spectra (Table 1) were recorded in solution on a Perkin–Elmer Paragon 1000 FT spectrophotometer. NMR spectra (Table 2) were run on Bruker DPX-300 (room temperature) and AMX-400 (low temperature) instruments, using the residual solvent peak (for ^{1}H) or external 85% H_3PO_4 (for ^{31}P) as references. Microanalyses were obtained from the University of Oviedo Analytical Service. FAB MS were obtained from the University of Santiago de Compostela Mass Spectrometric Service; data given refer to the most abundant molecular ion isotopomer.

4.2. Synthesis of $[Ru_3(\mu\text{-}H)(\mu_3\text{-}HNNMe_2)(CO)_9]$ (**1**)

A solution of $[Ru_3(CO)_{12}]$ (1.000 g, 1.560 mmol) and H_2NNMe_2 (500 μl, 8.32 mmol) in THF (70 ml) was stirred at reflux temperature for 3 h. The color changed from orange to dark brown. The solvent was removed under reduced pressure and the residue was dissolved in the minimum volume of THF. This solution was transferred into a chromatography column of neutral alumina (activity III, 2 × 20 cm) packed in hexane. Hexane eluted a small amount of unreacted ruthenium carbonyl. Dichloromethane–hexane (1:1) eluted the product, which was obtained as a yellow solid upon solvent removal (376 mg, 39%). A dark residue remained uneluted at the top of the column. *Anal.* Found: C, 21.93; H, 1.41; N, 4.47. Calc. for $C_{11}H_8N_2O_9Ru_3$: C, 21.46; H, 1.31; N, 4.55%. FAB MS (*m*/*z*): 617 [M^+].

4.3. Synthesis of $[Ru_3(\mu\text{-}H)_2(\mu_3\text{-}HNNMe_2)(CO)_9][BF_4]$ (**2**)

One drop (from a Pasteur pipette) of a 54% solution of $H[BF_4]$ in diethyl ether was added to a solution of compound **1** (50 mg, 0.081 mmol) in dichloromethane (5 ml). The solvent was removed under reduced pressure and the residue was washed with diethyl ether (3 × 5 ml) and dried in vacuo to give complex **2** as a pale yellow solid (49 mg, 87%). *Anal.* Found: C, 18.57; H, 1.26; N, 3.67. Calc. for $C_{11}H_9BF_4N_2O_9Ru_3$: C, 18.79; H, 1.29; N, 3.98%. FAB MS (*m*/*z*): 618 [$M^+ - BF_4$].

4.4. Reaction of compound *1* with triphenylphosphane

PPh_3 (24 mg, 0.089 mmol) was added to a solution of compound **1** (50 mg, 0.081 mmol) in THF (30 ml). The solution was stirred at reflux temperature for 30 min. The solvent was removed under reduced pressure and the oily residue was stirred in hexane (15 ml) to give a yellow solid (53 mg, 78%), subsequently identified by IR and NMR (^1H and ^{31}P) as an approximately 50% mixture of complexes **3a** and **3b**.

4.5. Synthesis of $[Ru_3(\mu\text{-}H)(\mu_3\text{-}HNNMe_2)(PPh_3)(CO)_8]$ (*3a*)

Triethylamine (8 μl, 0.057 mmol) was added to a solution of complex **4a** (40 mg, 0.043 mmol) in dichloromethane (20 ml). After stirring for 30 min, the solvent was removed under reduced pressure and the residue was purified by column chromatography on neutral alumina (activity III, 2 × 10 cm). Hexane–dichloromethane (2:1) eluted a yellow band that yielded compound **3a** as a yellow solid after solvent removal (21 mg, 57%). *Anal.* Found: C, 40.16; H, 2.82; N, 3.09. Calc. for $C_{28}H_{23}N_2O_8PRu_3$: C, 39.58; H, 2.73; N, 3.30%. FAB MS (*m*/*z*): 851 [M^+].

4.6. Synthesis of $[Ru_3(\mu\text{-}H)_2(\mu_3\text{-}HNNMe_2)(PPh_3)(CO)_8][BF_4]$ (*4a*)

PPh_3 (20 mg, 0.078 mmol) was added to a solution of compound **2** (50 mg, 0.071 mmol) in THF (30 ml). The solution was stirred at reflux temperature for 20 min. The solvent was removed under reduced pressure and the oily residue was washed with diethyl ether (2 × 6 ml) and dried in vacuo to give complex **4a** as a yellow solid (64 mg, 96%). *Anal.* Found: C, 36.02; H, 2.66; N, 2.78. Calc. for $C_{28}H_{24}BF_4N_2O_8PRu_3$: C, 35.87; H, 2.58; N, 2.99%. FAB MS (*m*/*z*): 852 [$M^+ - BF_4$].

4.7. Protonation of *3a*+*3b* with tetrafluoroboric acid

Two drops (from a Pasteur pipette) of a 54% solution of $H[BF_4]$ in diethyl ether was added to a dichloromethane (5 ml) solution containing 50 mg of a 1:1 mixture of compounds **3a** and **3b**. The solvent was removed under reduced pressure and the residue was washed with diethyl ether–hexane (1:1, 2 × 5 ml) to give a yellow solid (38 mg, 86%), subsequently identified by IR and NMR (^1H and ^{31}P) as an approximately 1:1 mixture of compounds **4a** and **4b**.

4.8. X-ray structure determinations of *2* and *4a*

X-ray intensity data were collected with a Nonius KappaCCD diffractometer. The structures were solved by Patterson methods with DIRDIF-96 [11] and refined with SHELX-97 [12] against F^2 of all reflections. Empirical absorption corrections were applied using XABS2 [13]. Two crystallographically independent molecules were found in the crystal of compound **2**. All non H-atoms were refined anisotropically. The hydrogen atoms H1A, H2A and H2B of **2** and H1 and H10 of **4a** were located in the corresponding Fourier maps and their coordinates and thermal parameters were refined. The position of the hydride atoms H1B of **2** and H2 of **4a** were calculated using the program XHYDEX [14], their coordinates were fixed and their thermal parameters were refined. The remaining hydrogen atom positions were calculated riding on their parent atoms. The drawings and structure calculations were performed with PLATON [15]. The WINGX program package was used throughout the structure determinations [16]. A selection of crystal and refinement details is given in Table 4.

5. Supplementary material

Complete crystallographic data for compounds **2** and **4a** have been deposited with the Cambridge Crystallographic Data Center, CCDC Nos. 184271 and 184272, respectively. Copies of this information may be obtained free of charge from The Director, CCDC, 12 Union Road, Cambridge, CB12 1EZ, UK (fax: +44-1223-336-033; e-mail: deposit@ccdc.cam.ac.uk or http://www.ccdc.cam.ac.uk).

Acknowledgements

Financial support form the Spanish DGESIC (grants PB98-1555 to J.A.C., and BQU2000-0219 to S.G.-G.) is gratefully acknowledged.

References

[1] For reviews on general reactivity of triruthenium carbonyl clusters, see: M.I. Bruce, In: G. Wilkinson, F.G.A. Stone, E.W. Abel (Eds.), Comprehensive Organometallic Chemistry, vol. 4, Pergamon, London, 1982, p. 843;
(b) M.I. Bruce, Coord. Chem. Rev. 76 (1987) 1;
(c) A.J. Deeming, in: E.W. Abel, F.G.A. Stone, G. Wilkinson, D.F. Shriver, M.I. Bruce (Eds.), Comprehensive Organometallic Chemistry II, vol. 7, Pergamon, London, 1995, p. 683.
[2] J.A. Cabeza, I. del Río, V. Riera, S. García-Granda, S.B. Sanni, Organometallics 16 (1997) 3914.
[3] P.L. Andreu, J.A. Cabeza, V. Riera, C. Bois, Y. Jeannin, J. Chem. Soc., Dalton Trans. (1990) 3347.
[4] P.L. Andreu, J.A. Cabeza, M.A. Pellinghelli, V. Riera, A. Tiripicchio, Inorg. Chem. 30 (1991) 4611.
[5] P.L. Andreu, J.A. Cabeza, V. Riera, Inorg. Chim. Acta 186 (1991) 225.
[6] P.L. Andreu, J.A. Cabeza, J.L. Cuyás, V. Riera, J. Organomet. Chem. 427 (1992) 363.

[7] S. Alvarez, P. Briard, J.A. Cabeza, I. del Río, J.M. Fernández-Colinas, F. Mulla, L. Ouahab, V. Riera, Organometallics 13 (1994) 4360.
[8] T. Jemke, H. Stoeckli-Evans, G. Süss-Fink, J. Organomet. Chem. 391 (1990) 395.
[9] B. Hansert, H. Vahrenkamp, Chem. Ber. 126 (1993) 2017.
[10] H. Günther, NMR Spectroscopy, Wiley, New York, 1980, p. 243.
[11] P.T. Beurskens, G. Beurskens, W.P. Bosman, R. de Gelder, S. García-Granda, R.O. Gould, R. Israël, J.M.M. Smits, The DIRDIF-96 Program System, Crystallography Laboratory, University of Nijmegen, Nijmegen, The Netherlands, 1996.
[12] G.M. Sheldrick, SHELXL-97, Version 97-2, University of Göttingen, Göttingen, Germany, 1997.
[13] S. Parkin, B. Moezzi, H. Hope, J. Appl. Crystallogr. 28 (1995) 53.
[14] A.G. Orpen, J. Chem. Soc., Dalton Trans. (1980) 2509.
[15] A.L. Spek, in: D. Sayre (Ed.), Computational Crystallography, Clarendon Press, Oxford, 1982, p. 528.
[16] L.J. Farrugia, J. Appl. Crystallogr. 32 (1999) 837.